Interaction of phospholipid vesicles with smooth metal-oxide surfaces

Gábor Csúcs [a], Jeremy J. Ramsden [b,*]

[a] Institute of Biochemistry, University of Zürich, Winterthurerstr. 190, CH-8057 Zürich, Switzerland
[b] Department of Biophysical Chemistry, Biozentrum, Klingelbergstr. 70, CH-4056 Basel, Switzerland

Abstract

The interaction of phospholipid vesicles with planar metal oxide supports has been previously reported as a means of preparing supported lipid bilayers, which are useful models of biological membranes. Nevertheless, extant evidence that bilayers are actually formed is rather circumstantial, and the necessary and sufficient conditions for their formation have never been delineated. Here, we tackle this problem by using smooth planar optical waveguides as the support. Analysis of the lightmode spectra of the waveguides, measured in situ during the deposition process, yields the mass of lipid deposited at the solid/liquid interface. By comparing the optogeometric parameters of the structures assembled from the vesicles with those of a lipid bilayer of known structure assembled using the Langmuir–Blodgett technique, we show that in many cases the vesicles remain intact and form a supported layer of vesicles rather than a bilayer, and often mixed structures (intact vesicles embedded in a bilayer partially covering the surface) occur. Careful analysis of the lipid deposition kinetics corroborates this result. We have also found that divalent cations dramatically promote attachment of mixed phosphatidylcholine/phosphatidylglycerol vesicles to form supported vesicle layers, and bilayer formation from pure phosphatidylcholine vesicles. © 1998 Elsevier Science B.V.

Keywords: Divalent cation; Kinetics; Optical waveguide lightmode spectroscopy (OWLS); Phospholipid; Planar bilayer; Vesicle

1. Introduction

Supported phospholipid bilayers are widely used as models for cell membranes. If the support is a hydrophilic hydrated metal oxide (e.g. silica), the presence of water layers between the support and the bilayer [1] ensures that the membrane retains cell-like fluidity. The lipids can be either pure substances or extracts from natural membranes.

The standard method of preparing such bilayers is via the Langmuir–Blodgett and Langmuir–Schaefer techniques [2,3]. Although they have the advantage of generating well-defined, known structures, it is not always practicable to use them: for example, they cannot be used when the bilayer must be deposited on the inside of a glass tube.

Several literature accounts refer to an alternative way of preparing supported bilayers by bringing a suspension of vesicles into contact with the support. They usually quote an article by Brian and Mc-Connell [4], who labelled some of their lipids by fluorescent markers, and merely state that "uniform fluorescent membranes are formed when the vesicle

---

* Corresponding author. Fax: 4161 267 2189.

suspension contains lipids at 2, 0.2 or 0.2 mM, but not when the vesicle suspension contains 0.01 mM lipids. The fluorescent membrane appears uniform with occasional small vesicles attached.'' It was not possible to ascertain whether a monolayer, bilayer or multilayer was formed. An indirect measurement of Horn [5], who determined the separation of vesicle-coated mica surfaces when pushed together, suggested that the vesicles were disrupted to form bilayers. The first direct quantitative attempt to understand the process of vesicle deposition on solid surfaces was reported by Jackson et al. [6], who measured the adsorption of lipid from vesicle dispersions onto glass beads by a batch procedure using a radiochemical assay. Their results suggested that a lipid monolayer is formed at the glass/water interface, and that the delivery of lipid to the interfaces takes place predominantly via vesicles rather then via lipid monomer. The release of a soluble fluorescent marker from within the vesicles was used to show that the vesicles were disrupted upon deposition. Nollert et al. [7], using an assay in which 1% of the lipids were fluorescently labelled [1], established that, depending on the lipid type, a supported layer of intact vesicles (SLV) could be formed, and found evidence that bilayer formation was nucleated by morphological heterogeneities (roughness) at the surface. Our aim, here, is to find the conditions under which bilayer formation can take place (if at all), using an integrated optical (reflectometric) technique, optical waveguide lightmode spectroscopy (OWLS), to determine the absolute mass of lipid deposited to a precision of ± 1 ng/cm^2. There is no perturbation of the lipids due to fluorescent or radiochemical labelling. Deposition was carried out from a vesicle suspension flowing over the substrate under precisely controlled hydrodynamic conditions, and the lightmode spectra measured with a time resolution of 30 s per point or less. This enabled the deposition kinetics to be quantitatively analyzed. The steady structures formed were compared with Langmuir–Blodgett films of known structure.

---

[1] Unfortunately it is not easy to reliably determine the absolute amount of deposited lipid from the measured fluorescent intensity, due to uncertainties in the quantum yield, etc.

2. Materials and methods

2.1. Chemicals

Synthetic 1-palmitoyl-2-oleoyl-sn-glycero-3-phosphatidylcholine (POPC) and 1-palmitoyl-2-oleoyl-sn-glycero-3-phosphatidylglycerol (POPG) were purchased from Avanti (Alabaster, Alabama) and used without further purification. All other chemicals were analytical grade reagents from Fluka (Buchs, St. Gallen). Water was doubly distilled; 10 mM 4-(2-hydroxyethyl)-piperazine-1-ethane-sulphonic acid (Fluka)-NaOH, pH 7.3 buffer was used throughout, i.e. for presoaking the waveguides, as the subphase during the LB deposition, and for preparing the vesicles.

2.2. Optical waveguides

Planar optical waveguides (''chips'') of composition $Si_{0.76}Ti_{0.24}O_2$ made by oxidative sputtering from a Si–Ti target, and incorporating a grating coupler (grating constant $\Lambda = 714.29$ nm) were obtained from Artificial Sensing Instruments, Zurich (type 1400). Their mean surface roughness was determined by atomic force microscopy to be 0.12 nm. Prior to use, the chips were refluxed in hot ethanol in a Soxhlet extractor for one hour, extensively rinsed with distilled water, and stored overnight in buffer. After each experiment the chips were cleaned by:
1. slowly lowering vertically into the LB trough, the surface of which had been freshly cleaned, thus removing most of the lipids from the surface [8], and
2. refluxing as described above.

2.3. Vesicle preparation.

An initial suspension of large multilamellar vesicles (LMV) was made by placing a solution of the lipid in chloroform into a glass flask and evaporating the solvent at room temperature under reduced pressure while rotating the flask. The solvent-free lipid film was kept under high vacuum for one hour and the LMV then generated by adding buffer solution and vortexing.

Sonified unilamellar vesicles (SUV) were prepared in the laboratory of H. Hauser (ETH Zurich) by immersing an ultrasonic tip in the suspension of LMV (10–15 mg/ml) for 30 min under a nitrogen atmosphere in a cold room. The lipid solution was continuously cooled in an ice bath, thus preventing boiling of the liposome suspension. Metal particles detached from the tip were removed by centrifuging. The resulting SUV had a mean diameter of 25 nm, as checked by quasi-elastic light scattering.

To make extruded vesicles (EV), after five freeze–thaw cycles the LMV suspension was extruded ten times through a 100 nm pore-size polycarbonate filter (Nucleopore, Pleasanton, CA). The radius R of the vesicles was determined by quasi-elastic light scattering to be 45 ± 3 nm. Final lipid concentrations of the vesicle suspensions were estimated from the nominal lipid stock solution concentrations supplied by the manufacturer. We did not attempt to quantify lipid losses during the various stages of vesicle preparation, because both the amount of deposited lipid at saturation and the type of kinetics appeared to be insensitive to bulk lipid concentration over a wide range (estimated as 0.2–4 mM).

2.4. Langmuir–Blodgett (LB) lipid deposition

Essentially, standard Langmuir–Blodgett (LB) and Langmuir–Schaefer (LS) techniques were used [2,3]. The desired lipid was dissolved in a 9 : 1 :: hexane : ethanol solution to give an ~ 1 mM solution, and spread on the surface of a laboratory-built Langmuir trough ($150 \times 10 \times 35$ mm) filled with buffer. After waiting five minutes for the lipid sol-

vent to evaporate, the layer was slowly compressed to a surface pressure of 32 mN/m. The waveguide, which had been previously lowered into the subphase before spreading the lipid, was now slowly (0.102 mm/s) raised vertically, while keeping the surface pressure constant via electronic feedback between the filter paper Wilhelmy plate monitoring the surface pressure and the motor driving the moving barrier. This resulted in a lipid monolayer on the surface of the waveguide. To form a bilayer on the waveguide, it was gripped in tweezers and lowered rapidly by hand parallel to and through the floating monolayer into a receptacle on the floor of the trough.

2.5. Optical waveguide lightmode spectroscopy (OWLS)

A small cylindrical flow-through cuvette was sealed to the waveguide with an 'o'-ring, such that the waveguide formed one wall of the cuvette. The assembly was then transferred to the measuring head of an IOS-1 integrated optical scanner (Artificial Sensing Instruments, Zurich). In this instrument, a monochromatic, linearly polarized light beam (He–Ne laser, wavelength $\lambda = 632.82$ nm) is directed onto the grating coupler area of the chip, and the angle α between the grating normal and the incident beam varied to microradian precision by a computer-driven stepping motor. At certain discrete angles, the light couples into the waveguide and is detected with photodiodes positioned at the ends of the waveguide [9]. The angles corresponding to the coupling maxima are then used to calculate the effective refractive indices N of the transverse electric (TE) and trans-

Table 1
Characteristics of the experiments

Type of experiment	Substrate	Vesicles			Divalent cations
		lipid	method	R (nm)	
1	Si(Ti)O$_2$	POPC	extrusion	45	
2	Si(Ti)O$_2$	POPC	sonication	12.5	
3	POPC monolayer	POPC	extrusion	45	
4	Si(Ti)O$_2$	POPC	extrusion	45	Ca^{2+} or Mg^{2+}
5	Si(Ti)O$_2$	POPC/POPG	extrusion	45	
6	Si(Ti)O$_2$	POPG/POPG	extrusion	45	Ca^{2+} or Mg^{2+}

verse magnetic (TM) modes, according to the incoupling relation [10]:

$$N = n\sin \alpha + \ell\lambda/\Lambda \qquad (1)$$

where n is the refractive index of air and ℓ is the diffraction order. At the beginning of a measurement

run, pure buffer was drawn through the cuvette in order to determine the optogeometric parameters of the waveguiding film F, i.e. refractive index n_F and thickness d_F, by solving the three-layer mode equations [10]. The refractive index n_C of the buffer solution covering the waveguide was measured with an LI3 Rayleigh interferometer (Carl Zeiss, Jena).
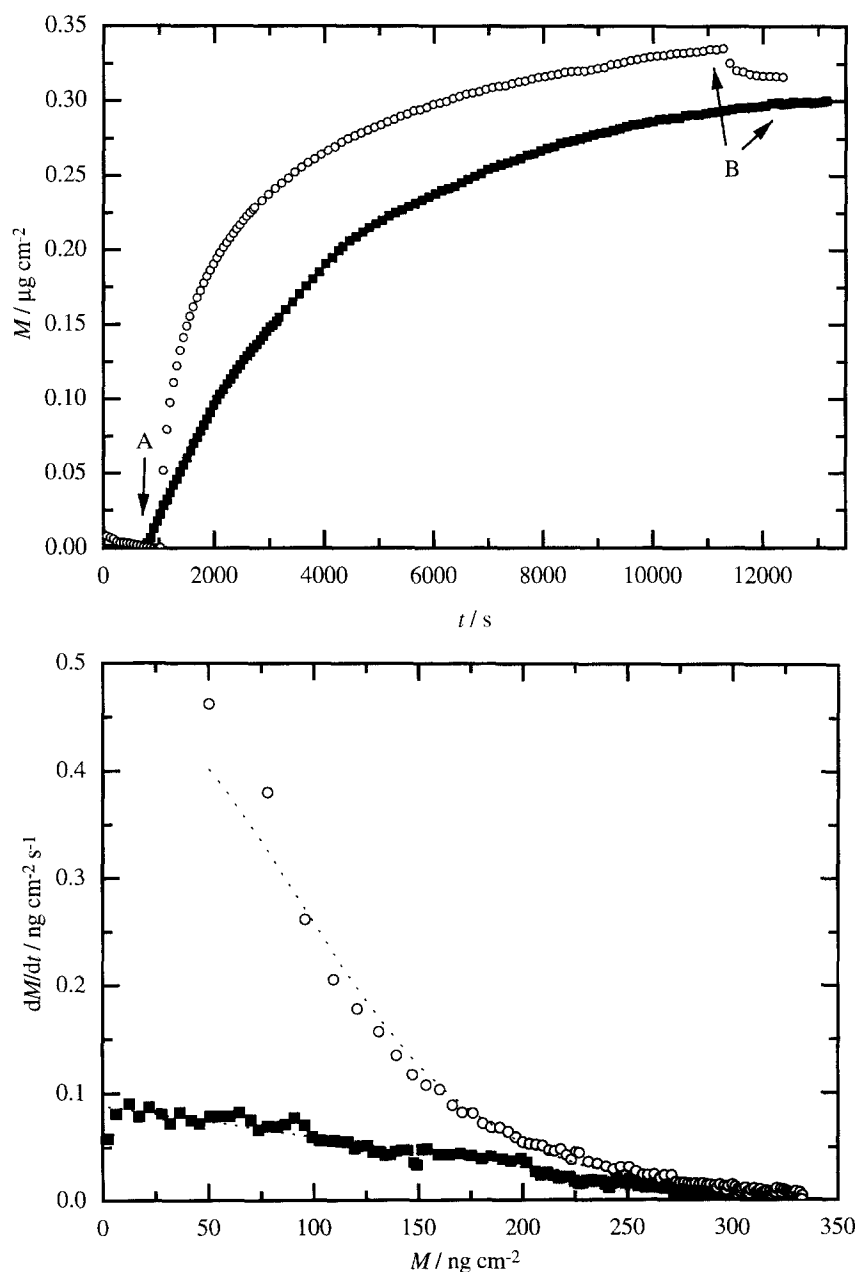

Fig. 1. (a) Adsorption of POPC vesicles leading to bilayer formation. (■) Langmuir and (○) RSA kinetics. Arrows A and B mark respectively the beginning and the end of vesicle flux. (b) The data of Fig. 1(a) replotted using the same symbols as the rate of deposition vs. the amount deposited. The dotted lines correspond to (■) Langmuir kinetics and (○) the Schaaf–Talbot polynomial.

The value of n_S, the refractive index of the C 7059 supporting glass, was provided by the manufacturer (Corning). Measurements were performed at room temperature.

After a stable baseline was established, the chip was either removed from the IOS-1 instrument in order to deposit an LB monolayer or an LB–LS bilayer and then replaced, or the buffer was substituted by a vesicle suspension, and measurement of the incoupling angles continued. The different types of experiments are enumerated in Table 1. The lipids deposited on the surface form an adlayer A whose thickness d_A and mean refractive index n_A can be found from the measured N_{TE} and N_{TM} by solving the four-layer mode equations [10]. In contact with pure buffer, the bilayers were stable indefinitely. The monolayers, however, were unstable [11], and hence flow was switched to the vesicle suspension after only a few minutes of baseline data collection.

2.6. Determination of the amount of deposited lipid

Since the thickness of an incomplete layer of adsorbed vesicles is a rather ill-defined quantity, we combined the two parameters n_A and d_A (determined experimentally as described and which we should,

perhaps, call "effective" or "mean" parameters), to find the mass M of lipid deposited per unit area, using the expression [12]:

$$M = d_A \frac{n_A - n_C}{\mathrm{d}n/\mathrm{d}c} \qquad (2)$$

where $\mathrm{d}n/\mathrm{d}c$ is the refractive index increment of the lipid material, M_2, the value of M for a bilayer, can be calculated precisely since the area a per lipid molecule in a monolayer of surface pressure 32 mN/m is known to be 0.72 nm^2 [13]; from the molecular weight of POPC (760 g/mol) the mass per molecule is 1.26×10^{-15} μg, and hence $M_2 = 0.35$ μg/cm^2, whence $\mathrm{d}n/\mathrm{d}c$ was determined as 0.083 cm^3/g.

3. Results

3.1. Extruded POPC vesicles on Si(Ti)O$_2$

Three types of adsorption behaviour were observed:

1. M_∞ (the adsorbed mass at saturation) was 0.33 ± 0.03 μg/cm^2, i.e. almost equal to M_2. The ad-
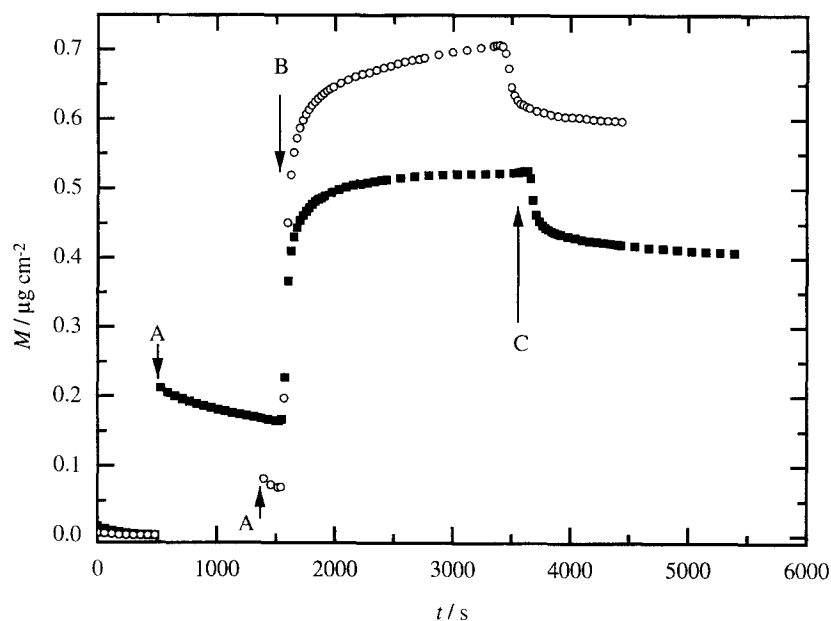

Fig. 2. Adsorption of POPC vesicles ([lipid] = 13 mM) to POPC monolayers deposited at a surface pressure of 32 mN/m. The adsorbed mass is higher when the monolayer is "imperfect" (i.e. (O) $M_{monolayer} < 0.18$ μg/cm^2) compared with a "perfect" monolayer ((■) $M_{monolayer} = 0.18$ μg/cm^2, see Section 3.3). Arrows: A – monolayer deposition, B – adding the vesicle solution, and C – washing with pure buffer.

sorption followed Langmuir kinetics, i.e. $M_\infty -$
$M(t) \sim e^{-t}$ (Fig. 1(a)). When pure buffer replaced
the vesicle suspension, no material was removed.
16% of experiments fell into this class (Fig. 1(a)
and (b)).

2. M_∞ (after washing) was $0.36 \pm 0.04\,\mu g/cm^2$,
which still corresponds to a bilayer, but the kinet-
ics were of the random sequential addition (RSA)

type [14]. The difference between Langmuir and
RSA kinetics is most easily seen in a plot of the
time derivative of M vs. M (Fig. 1(b)): Langmuir
behaviour gives a straight line, but RSA shows a
characteristic curvature. A small decrease ($\sim 5\%$
of M_{max}) in the adsorbed mass was observed upon
washing but thereafter the curve remained indefi-
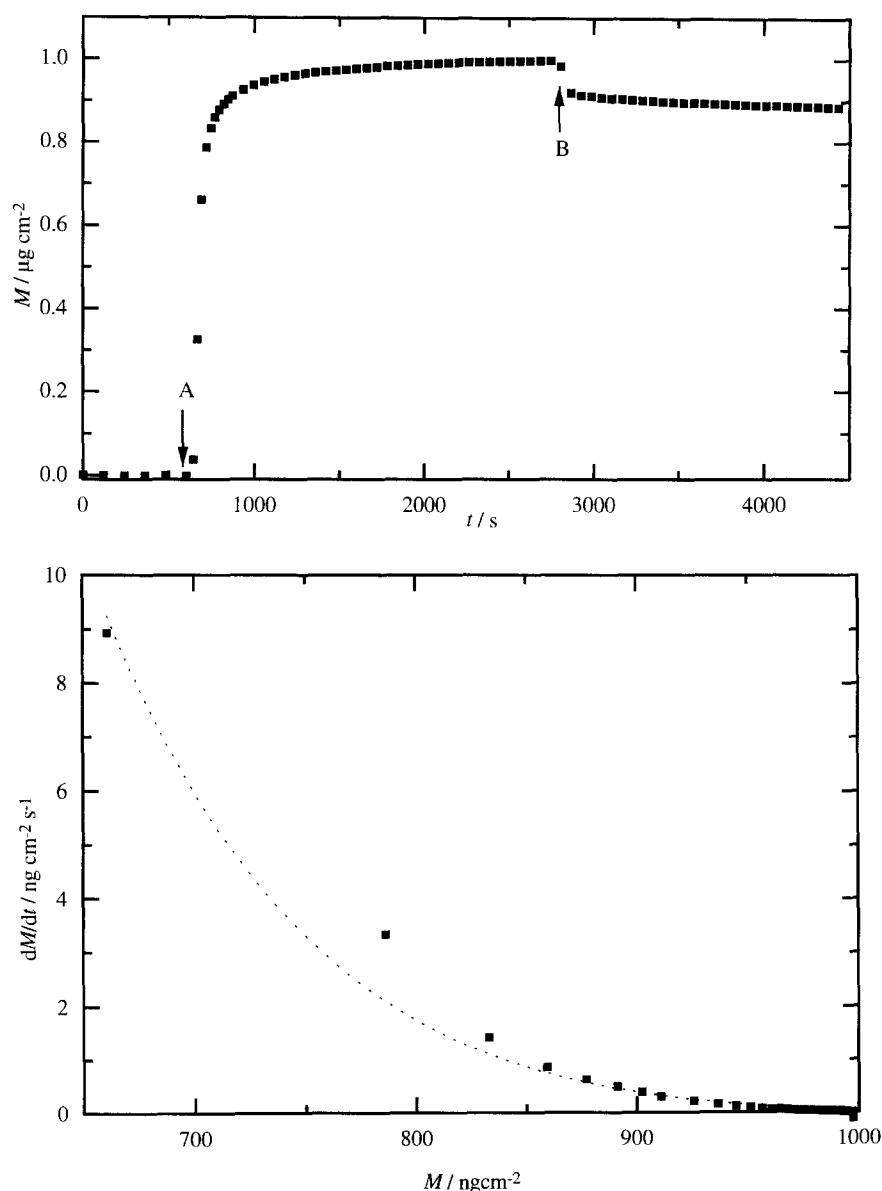nitely stable. Presumably, during washing loosely

Fig. 3. (a) Adsorption of extruded POPC/POPG (8:2) vesicles in the presence of 10 mM $CaCl_2$. Arrows: A – changing to vesicle solution, B – washing with buffer. (b) Kinetic evaluation of the data in 3(a), replotted and fitted by the Schaaf–Talbot polynomial.

Table 2
Summary of the experimental data

Type of experiment	% of experiments	M (μg cm^{-2})	M/M_2	Type of kinetics	Inferred result
1	16	0.33 ± 0.03	0.94	Langmuir	bilayer
1	40	0.36 ± 0.04	1.02	RSA	bilayer
1	44	0.62 ± 0.06	1.77	RSA	bilayer + vesicles
2	100	0.61 ± 0.04	1.74	RSA	bilayer + vesicles
3	100	0.40 ± 0.03	1.14	RSA	bilayer [a]
4	100	0.35 ± 0.04	1	RSA	bilayer
5	100	0	0	—	no deposition
6	100	0.89 ± 0.06	2.54	RSA	SVL + bilayer

[a] Depending on the quality of the monolayer, the adsorbed mass varied and, in some cases, a bilayer + vesicles structure was formed (see Section 3.3 and Fig. 2).

attached vesicles and other structures are washed away. Nearly 40% of the experiments showed this result.

3. The adsorbed amount was almost double M_2, $0.62 \pm 0.06\,\mu$g/cm^2, but the kinetics were still RSA-like. The decrease due to washing was $\sim$ 10%. It was found that 44% of the experiments fell into this group.

3.2. Sonicated POPC vesicles on Si(Ti)O$_2$

The sonicated vesicles showed only one type of behaviour, corresponding to Item 3 in Section 3.1. Compared to the extruded ones, much smaller (ca. 1/10) lipid concentrations were enough to give a similar rate of deposition. The adsorption kinetics were never Langmuirian, but resembled the RSA pattern. M_∞ was $0.61 \pm 0.04\,\mu$g/cm^2, ~ 1.8 times more than for a bilayer. Washing had no effect on the adsorbed mass.

3.3. Extruded POPC vesicles on POPC monolayers

The adsorbed amount of lipid depended on the the quality of the monolayer (Fig. 2). If the mass of the monolayer was close to ideal (i.e. $M = 0.18\,\mu$g/cm^2), then M_∞ was $0.4\,\mu$g/cm^2, close to that expected for a bilayer. If the monolayer was less perfect (i.e. $M < 0.18\,\mu$g/cm^2), then the adsorbed mass at the end was $0.6\,\mu$g/cm^2, about twice that expected for a bilayer. Adsorption in both cases followed RSA kinetics, and washing reduced the adsorbed mass by 20%.

3.4. Effect of divalent cations on adsorption

Ca^{2+} and Mg^{2+} had a dramatic effect on the rate of adsorption of extruded POPC vesicles, accelerating the adsorption process about tenfold, independently of the salt concentration (1 or 10 mM) and nature (CaCl$_2$ or MgCl$_2$). In most cases, the adsorbed mass was $0.35 \pm 0.04\,\mu$g/cm^2, almost equal to a bilayer. The adsorption kinetics were always of the RSA type, and washing removed 20% of the adsorbed mass.

3.5. POPG / POPC vesicle adsorption

To further study the effect of electrostatic charges on the adsorption process (particularly since negatively charged lipids are often present in natural biological membranes), we incorporated 20% POPG into the POPC vesicles. In the absence of divalent cations no adsorption could be detected [2]. In the presence of 10 mM CaCl$_2$ or MgCl$_2$, the adsorbed mass at saturation was three times larger than M_2, and after washing was it was $0.89 \pm 0.06\,\mu$g/cm^2, still two-and-a-half times greater. The mass after washing was 15% less than the maximum mass, which on an absolute scale was the largest mass difference observed. A typical measurement and corresponding kinetic evaluation curve are shown in Fig. 3.

The results are summarized in Table 2.

---

[2] Note that, at the pH of all experiments, the waveguides are weakly negatively charged. Their surface potential, calculated according to the Healy–White [15] model, was -95 mV.

4. Discussion

We consider the following four cases:

1. The vesicles arriving at the uncoated chip surface are disrupted and form a bilayer. M is the same as for an LB–LS bilayer. We call this value M_2.

2. The arriving vesicles stay intact and form a supported vesicle layer (SVL). If the vesicles were closely packed M would be four times higher than M_2, regardless of their radius R. Since, however, the vesicles are adsorbing on a continuum and do not interact with each other except via hard-body (insofar as the vesicles are "hard") interactions (the random sequential addition (RSA) model), at a fractional surface coverage of only 0.55, the surface will be already jammed, i.e. no gaps large enough to accomodate a single further vesicle remain [16]. Hence, $M = 2.2\,M_2$.

3. The arriving vesicles are flattened, but stay intact: in this case M depends on the degree of flattening. Here again the RSA model was used. Clearly M is greatest for the unflattened vesicles (Item 2 above) and lowest for the completely flattened vesicles ($M = 1.1\,M_2$).

4. The arriving vesicles partially fuse to form an incomplete bilayer, but some stay intact and sit in holes of the bilayer. Here, the vesicles can also be flattened. There are two possible models to calculate the mass/area ratio of these systems. Let x be the fraction of the surface occupied by vesicles; $x \leq 0.55$ (see Item 2 above). Hence

$$M/M_2 = (1 - x) + 4x, \qquad (3)$$

i.e. gaps in the bilayer are filled by vesicles. A second, perhaps more realistic, model takes the difference between the thickness of the bilayer

(5 nm) and the size of the vesicles into account (for example, an $R = 45$ nm vesicle needs a circular gap of only 20 nm radius in order to be adsorbed), i.e.

$$M/M_2 = (1 - x) + 0.8x + 4x, \qquad (4)$$

where the factor 0.8 is specific for (extruded) $R = 45$ nm vesicles.

The results from these calculations are summarized in Table 3.

4.1. Kinetics

Adsorption will follow Langmuir kinetics when the RSA exclusion zones are annihilated. An obvious mechanism for this to occur involves the vesicles being rapidly (compared to the time necessary for their attachment to the surface) disrupted after arriving at the surface [6]. If, on the other hand, the vesicles arriving at the surface are not immediately fused or otherwise disrupted, RSA kinetics will be observed. Ultimate fusion is not ruled out, but disruption (and any associated process, such as lipid rearrangement) is slower than the rate at which vesicles arrive at the surface; in other words, the vesicles first form an SVL, and may later fuse to form a bilayer. Hence, vesicles and bilayer structures are both present, as has been observed with atomic force microscopy [17].

The kinetic analysis can be taken still further. The general kinetic equation describing the deposition of matter at the solid/liquid interface is:

$$dM/dt = k_a c_1 \phi \qquad (5)$$

where k_a is the adsorption rate coefficient and c_1 the concentration of the adsorbing entity in the vicinity

Table 3

Predicted M values. Pure POPC and mixed POPC/POPG (8 : 2) vesicles and bilayers have practically identical values

Structure type	M (μm cm^{-2})	M/M_2
POPC bilayer	0.35	1
S(upported) v(esicle) l(ayer)	0.77	2.2
SVL (flattened vesicles)	0.39–0.77	1.2–2.2
Bilayer + 20% vesicles (Eq. (3))	0.56	1.6
Bilayer + 20% extruded vesicles (Eq. (4))	0.62	1.76
Bilayer + 20% sonicated vesicles (Eq. (4))	0.59	1.68
SVL (extruded) + 45% bilayer (maximal mass) (Eq. (4))	1.08	3.09
SVL (completely flattened) + 45% bilayer (Eq. (4))	0.86	2.45

Table 4
Summary of the fitted kinetic parameters

Type of experiment	% of experiments	Fitted a/m values ($cm^2/\mu g$)	Fitted $k_a c_1$ values ($\mu g/cm^2\, s^{-1}$)	Fitting quality
1[a]	16	0.77	3.8	good
1	40	1.98	15	poor
1	44	0.83	14.4	good
2	100	0.73	9.9	poor
3	100	0.86	0.09	good
4	100	1.34	2.6	poor
6	100	0.53	0.07	good

[a] Langmuir kinetics.

of the surface, and ϕ the fraction of the surface still unoccupied by matter. Schaaf and Talbot have provided an accurate interpolation formula giving ϕ as a function of θ, the fraction of the surface occupied (Eq. 42 of Ref. [14]). With the help of the following relation:

$$\theta = Ma/m, \tag{6}$$

where a and m are, respectively, the area occupied and mass per adsorbing entity, we can fit Eq. (5) to the dM/dt vs. M data using two independent free parameters, the quotient a/m and the product $k_a c_1$. Using the foregoing data (at the end of Item 2), it is easy to calculate that, for a single lipid molecule, $a/m = 5.7\,\mu g/cm^2$, whereas for a 45 nm radius vesicle, we obtain $a/m = 0.7\,\mu g/cm^2$. The fitted parameters (Table 4)[3] show that the a/m values are generally very close to those expected for a vesicle, supporting the previous inference that transport is via vesicles rather than lipid monomers [6]. Further corroboration comes from the $k_a c_1$ values. Schwarz et al. [13] have found that the solubility of POPC in water is $\sim 10^{-8}$ M, i.e. $\sim 0.01\,\mu g/cm^2$. Taking this as the value of c_1, from the fitted $k_a c_1$ values, we then infer $k_a \approx 10\text{--}100\,cm/s$, whereas if c_1 is the concentration of vesicles ($\sim 0.2\,mg/cm^3$), we infer $k_a \approx 10^{-5}\text{--}10^{-4}\,cm/s$. The highest possible value of k_a (in the absence of an energy barrier retarding lipid adsorption) is $\sim D/\delta$, where D is the diffusivity and

δ the thickness of the diffusion boundary layer. For the vesicles, the Stokes–Einstein relation gives $D = 5.4 \times 10^{-8}\,cm^2/s$, and δ is estimated as $30\,\mu m$, hence $D/\delta \sim 10^{-5}\,cm/s$. For the lipid, we estimate $D/\delta \sim 10^{-4}\,cm/s$. Hence, the experimental data is only consistent with matter transport via vesicles.

4.2. Mixed SVL / bilayer formation

In 44% of the experiments, the adsorbed mass was on average 1.8 times more than expected for a bilayer. Comparing this fact with our theoretical calculations and taking into account the kinetic behaviour (RSA), we interpret it as resulting from 80% of the surface being covered by a bilayer, and the remaining 20% by vesicles or vesicle aggregates. This interpretation agrees with the previous observation that 80% of a lipid layer formed from vesicles had the lateral mobility characteristic of a true bilayer [18].

4.3. Deposition onto preformed lipid monolayers

Monolayer coverages of $< M_2/2$ (Section 3.3) probably mean that the monolayers are not perfectly continuous, i.e. holes can occur in the layer. We suggest that vesicles adsorbing to these holes stay intact while the vesicles arriving at the monolayer surface are disrupted and fuse with the monolayer to form a bilayer. In order to get a continuous bilayer by adsorption of vesicles to a monolayer, the quality of the initial monolayer is crucial.

4.4. Effect of divalent cations

The few published results on the effects of bivalent cations (mainly Ca^{2+}) on the vesicle adsorption pro-

---

[3] The fitting quality was best where SVL formation was deduced, and not so good where bilayers were ultimately formed, in which case the assumed ϕ function [14] for pure random sequential addition no longer corresponds to actuality.

cess are exiguous and somewhat ambiguous [7,18]. It is known that Ca^{2+} adsorbs to bilayers [19–21] and causes structural changes. These changes can lead to membrane (vesicle) fusion [22,23]. It appears, however, that appreciable fusion in the bulk vesicle suspension does not occur on the time scale of adsorption, as may be inferred from the a/m values (Table 4), which are consistent with the adsorption of intact single vesicles.

Prévost and Gallet [24] have hinted that Ca^{2+} may act by diminishing the normally repulsive hydration forces between lipid bilayers. This notion has since received further support from the experiments of Wu et al. [25].

5. Conclusions

Vesicles in the liquid crystalline phase brought into contact with a solid/liquid interface form planar bilayers rather than monolayers or supported vesicle layers. Nevertheless, under typical conditions, a mixture of bilayers and intact vesicles is formed, rather than pure bilayers. These conclusions have been reached by:

- comparing the optogeometric parameters of the structures formed from vesicles with those of LB–LS films of known structure, and
- from the analysis of the deposition kinetics.

Lipid deposition is accelerated by the presence of divalent cations.

Acknowledgements

References

[1] S.J. Johnson, T.M. Bayerl, D.C. McDermott, G.W. Adam, A.R. Rennie, R.K. Thomas, E. Sackmann, Biophys. J. 59 (1991) 289–294.
[2] K.B. Blodgett, I. Langmuir, Phys. Rev. 51 (1937) 964–972.
[3] I. Langmuir, V.J. Schaefer, J. Amer. Chem. Soc. 60 (1937) 1351–1360.
[4] A.A. Brian, H. McConnell, PNAS 81 (1984) 6159–6163.
[5] R.G. Horn, Biochim. Biophys. Acta 778 (1984) 1224–1228.
[6] S. Jackson, M.D. Reboiras, I.G. Lyle, M.N. Jones, Faraday Discuss. Chem. Soc. 85 (1986) 291–301.
[7] P. Nollert, H. Kiefer, F. Jaehnig, Biophys. J. 69 (1995) 1447–1455.
[8] I. Langmuir, Faraday. Trans. Chem. Soc. 15 (1919) 62–74.
[9] K. Tiefenthaler, Adv. Biosensors 2 (1992) 261–289.
[10] K. Tiefenthaler, W. Lukosz, J. Opt. Soc. Amer. B 6 (1989) 209–220.
[11] V.V. Yaminski, P.M. Claesson, J.C. Eriksson, J. Colloid Interface Sci. 161 (1993) 91–100.
[12] J.A. de Feijter, J. Benjamins, F.A. Veer, Biopolymers 17 (1978) 1759–1772.
[13] G. Schwarz, G. Wackerbauer, S.E. Taylor, Coll. Surfaces A111 (1996) 39–47.
[14] P. Schaaf, J. Talbot, J. Chem. Phys. 91 (1989) 4401–4409.
[15] T.W. Healy, L.R. White, Adv. Coll. Interface Sci. 9 (1978) 303–345.
[16] E.L. Hinrichsen, J. Feder, T. Jøssang, J. Statist. Phys. 44 (1986) 793–827.
[17] I. Vikholm, J. Peltonen, O. Teleman, Biochim. Biophys. Acta 1233 (1995) 111–117.
[18] E. Kalb, S. Frey, L.K. Tamm, Biochim. Biophys. Acta 1103 (1992) 307–316.
[19] L.J. Lis, V.A. Parsegian, R.P. Rand, Biochem. 20 (1981) 1761–1770.
[20] L.J. Lis, W.T. Lis, V.A. Parsegian, R.P. Rand, Biochem. 20 (1981) 1771–1777.
[21] R. Lehrmann, J. Seelig, Biochim. Biophys. Acta 1189 (1994) 89–95.
[22] S. Ohki, Biochim. Biophys. Acta 689 (1982) 1–11.
[23] D. Papahadjopoulos, S. Nir, N. Düzgünes, J. Bioener. Biomembr. 22 (1990) 157–179.
[24] M. Prévost, D. Gallez, Faraday Trans. Chem. Soc. 80 (1983) 517–533.
[25] W. Wu, R.F. Giese, C.J. van Oss, Coll. Surf. A 89 (1994) 241–252.